ELSEVIER

Bioelectrochemistry 58 (2002) 75–85

Bioelectrochemistry

www.elsevier.com/locate/bioelechem

Structural and thermodynamic features of complexes formed by DNA and synthetic polynucleotides with dodecylamine and dodecyltrimethylammonium bromide

A.I. Petrov [a,*], D.N. Khalil [b], R.L. Kazaryan [a], I.V. Savintsev [a], B.I. Sukhorukov [a]

[a] *Institute of Theoretical and Experimental Biophysics Russian Academy of Sciences, Pushchino, Moscow Region, 142290 Russia*
[b] *Great Neck North High School, New York, 42 Red Brook Road, Great Neck, NY 11024, USA*

Received 14 June 2001; received in revised form 8 December 2001; accepted 11 January 2002

Abstract

Complex formation of native and denatured DNA, single-stranded polyribonucleotides poly(A) and poly(U), as well as double-stranded poly(A)·poly(U) with dodecylamine (DDA) and dodecyltrimethylammonium bromide (DTAB) has been studied by UV-, CD-, IR-spectroscopy and fluorescence analysis of hydrophobic probe pyrene. DDA and DTAB were shown to bind cooperatively with DNA and polyribonucleotides, resulting in the formation of complexes containing hydrophobic micelle-like clusters. Critical aggregation concentration (CAC) of DDA and DTAB shifts sharply to lower values (30–50 times) in the presence of DNA and polynucleotides as compared to critical micelle concentration (CMC) of free DDA and DTAB in solution. The analysis of binding isotherms within the frame of the model of cooperative binding of low-molecular ligands to linear polymers allowed us to determine the thermodynamic parameters of complex formation and estimate the contribution of electrostatic interaction of positively charged heads of amphiphiles with negatively charged phosphate groups of DNA and polyribonucleotides, and hydrophobic interaction of aliphatic chains to complex stability. Electrostatic interaction was shown to make the main contribution to the stability of DNA complexes with DDA, while preferential contribution of hydrophobic interactions is characteristic of DTAB complexes with DNA. The opposite effect of DDA and DTAB on the thermal stability of DNA double helix was demonstrated from UV-melting of DNA—while DTAB stabilizes the DNA helix, DDA, to the contrary, destabilizes it. The destabilizing effect of DDA seems to originate from the displacement of intramolecular hydrogen bonds in complementary Watson–Crick A·T and G·C base pairs with intermolecular H-bonds between unsubstituted DDA amino groups and proton-accepting sites of nucleic bases.
© 2002 Elsevier Science B.V. All rights reserved.

Keywords: DNA; Polyribonucleotides; Cationic amphiphile; Fluorescence; Binding isotherm; Thermodynamics

1. Introduction

Complexes of polyelectrolytes with oppositely charged surface-active amphiphilic molecules have been considered to be very intriguing colloidal systems "where physics, chemistry, biology and technology meet" [1]. It is not surprising therefore that the elucidation of physicochemical regularities of interactions in these systems, structural and thermodynamic features of the complexes is of great importance both from fundamental and practical viewpoints [2–12]. Complexes of natural polyanions—nucleic acids with cationic amphiphiles attract nowadays an increased attention. Their studies allow one to get a deeper insight into the molecular mechanisms of antiviral and antibacterial activity of cationic amphiphiles [13–15], physicochemical mechanisms of DNA compactization [16,17], DNA–membrane interactions [18–24], as well are important for working out the nucleic acid-based biosensors [25,26].

Powerful impetus to the studying the complexes of nucleic acids with cationic amphiphiles, or cationic lipids, which is simply another term used by biologically oriented researchers for cationic amphiphile, was given after revealing the ability of these complexes to facilitate the transfer of nucleic acids through biological membranes [27–35]. Such complexes are considered currently as very promising systems in gene therapy for functional gene delivery into eukaryotic cells; however, their transfection efficiency remains relatively low up to now in comparison with viral-

* Corresponding author. Tel: +7-967-790553; fax: +7-967-790553.
E-mail address: petrov@venus.iteb.serpukhov.su (A.I. Petrov).

1567-5394/02/$ - see front matter © 2002 Elsevier Science B.V. All rights reserved.
PII: S1567-5394(02)00130-5

based vectors [31]. It seems evident that accumulation of data on structure and physicochemical characteristics of DNA complexes with cationic amphiphiles differing in chemical structure of their hydrophobic tails and hydrophilic heads, and correlation of these data with transfection efficacy give us a way to reveal the algorithms for choosing among the great variety of cationic lipids, those of them possessing the highest DNA-delivering potential, and purposeful synthesis of such cationic lipids. Unsubstituted long-chain aliphatic amines and appropriate *N*-trialkylammonium salts can be considered as the simplest cationic lipids in this row.

Complexes of *N*-trimethylsubstituted derivatives of long-chain aliphatic amines (dodecyl-, tetradecyl-, and cetyltrimethylammonium bromide) with DNA have attracted the greatest attention of researchers [10,11,16,17,36–50], however, many questions of their physical chemistry remain to be cleared up. In particular, little is known about the effect of conformational state of DNA, rigidity of polynucleotide chain and its length, chemical structure of polar head of cationic amphiphile on the process of complex formation and many others.

In the present study, we have examined in detail the interaction of two cationic amphiphiles—dodecylamine (DDA) and dodecyltrimethylammonium bromide (DTAB), differing only in chemical structure of their hydrophobic heads: $-NH_3^{\oplus}$ in DDA and $-N(CH)_3^{\oplus}$ in DTAB, with DNA and synthetic polyribonucleotides using UV-, CD-, IR-, and fluorescence spectroscopy. Pyrene was chosen as hydrophobic fluorescent probe due to the high sensitivity of the fine vibronic structure of its emission spectra to the hydrophobicity of local environment [51–53].

2. Materials and methods

High molecular weight DNA (1.7×10^7 Da) isolated from sturgeon sperm by a standard procedure of phenol-chloroform extraction followed by ethanol precipitation was used in this study. DNA solution with concentration of 1.5–2 mg/ml was exhaustively dialyzed at 4 °C for 3 days against the solution of 10^{-2} M NaCl, 10^{-3} Tris–HCl, pH 7.2, which was taken as a standard buffer solution in all measurements. The concentration of DNA solutions was determined from UV absorption at 260 nm using the known molar extinction coefficient, 6600 M^{-1} cm^{-1} [54]. UV-melting temperature and hyperchromism of DNA were 69 °C and 40%, respectively, indicating the absence of double helix damaging during the process of DNA isolation. Denatured DNA preparations were obtained by boiling the buffer solution of DNA followed by rapid cooling with liquid nitrogen.

Polyuridylic and polyadenylic acids (poly(U) and poly(A), respectively) of Reanal (Hungary) were dialyzed for 3 days against twice distilled water and then liophilyzed. The concentrations of polynucleotides were determined from UV absorption using the following extinction coefficients $-\varepsilon_{260} = 9.2 \times 10^3$ M^{-1} cm^{-1} for poly(U) and $\varepsilon_{257} = 10.5 \times 10^3$ M^{-1} cm^{-1} for poly(A) [55]. Double-helical poly(A)·poly(U) was prepared by mixing equal volumes of equimolar solutions of poly(A) and poly(U) followed by heating the mixture up to 70 °C and slow annealing to room temperature.

DDA, DTAB and pyrene were purchased from Sigma-Aldrich Chemical (USA) and were used as received. The stock solution of pyrene was prepared in methanol of spectral purity grade by weighting, and the aliquots of this solution were added under thorough mixing to DNA solutions so that the final concentration of pyrene was 3×10^{-6} M and methanol concentration did not exceed 0.5% (by volume).

Fluorescence spectra of pyrene solutions were measured on a spectrofluorimeter Perkin-Elmer MPF-44B (USA) in 1-cm quartz cells at excitation wavelength 334 nm. All device settings such as slits of input and output monochromators, scanning rate, amplification and others were thoroughly controlled to exclude spectra distortions.

UV spectra were taken on UV–VIS spectrophotometer Specord-M40 (Zeiss, Germany), UV-melting profiles of DNA—on the spectrophotometer VSU-2P (Zeiss) supplied with a thermostated cell holder allowing to maintain the fixed temperature inside the cells with accuracy ± 0.5 °C within the range 13–97 °C.

IR-spectra (1800–950 cm^{-1}) of DNA complexes with DDA and DTAB, as well as the spectra of separate components of these complexes were taken on an infrared spectrophotometer Specord-M80 (Zeiss) at room temperature and relative humidity (r.h.) 93% when DNA exists in double-helical B-conformation. The samples of DDA, DTAB and DNA were prepared as thin films by evaporation of appropriate concentrated solutions on transparent calcium fluoride plates. Because of low solubility of complexes DNA–DDA and DNA–DTAB in water solutions, their samples for IR-measurements were prepared by consecutive, layer-by-layer, deposition of DNA and cationic amphiphile from water–saline solution (10 mM NaCl, pH 7.4) onto calcium fluoride plates. The procedure described by us elsewhere [56] is an extension of the method proposed earlier by Decher [57] for manufacturing organized inter-polyelectrolyte films made of alternating layers of positively and negatively charged polyelectrolytes.

CD spectra were measured on a spectropolarimeter Jasco-J500 (Japan). All the measurements were made immediately after sample preparation without incubation period.

3. Results and discussion

3.1. Fluorescent studies with pyrene as hydrophobic fluorescent probe

Pyrene is a flat aromatic molecule made of four condensed benzene rings. High symmetry of its chemical structure resulting in the absence of the net electric dipole

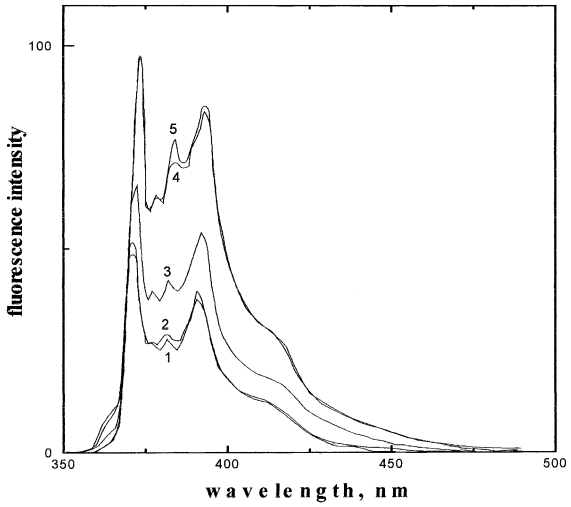

Fig. 1. Fluorescence spectra of pyrene (concentration 3×10^{-6} M) in 10^{-2} M NaCl, 10^{-3} M Tris–HCl, pH 7.2, in the absence of DDA and DTAB (2); (1, 5) at DDA concentrations, respectively, 5×10^{-4}M and 2×10^{-3} M in absence of DNA, and (3, 4) at DDA concentrations 2×10^{-4} M and 5×10^{-4} M, respectively, and DNA concentration 4.85×10^{-5} M (per phosphate residue).

momentum both in ground and excited state does not allow to wait for noticeable contribution of solvation effects into emission spectra of pyrene. Extensive experimental studies of pyrene fluorescence in a wide range of solvents (from water to hydrocarbons) [51,58,59] did not show any spectral shifts in solvents of different polarity. However, great perturbation with solvent polarity is really observed in the intensities of vibronic bands of fluorescence spectra of pyrene, which made this molecule an attractive tool for probing different hydrophobic systems.

Fig. 1 demonstrates fluorescence spectra of pyrene in buffer solution (10 mM NaCl, 1 mM Tris–HCl, pH 7.2) in the presence and absence of DDA and DNA. It is seen that the spectral parameters depend essentially both on the concentration of DDA, and on the presence and concentration of DNA. Similar spectral changes in pyrene fluorescence are also observed for DTAB. The most noticeable changes are observed in total intensity of vibronic bands in the range of wavelengths from 370 to 400 nm, in the ratio of intensities of vibronic bands at 372 and 383 nm, as well as in the presence or absence of the broad unstructured band with maximum at 470 nm and its intensity. The emission at 370–400 nm arises from the monomeric pyrene, while the band at 470 nm corresponds to the emission from pyrene excimers [42,59]. In principle, all these parameters may be used in analysis of hydrophobic systems (micelles, membranes, hydrophobic clusters and so on), but the ratio I_3/I_1, where I_1 and I_3 are the intensities of vibronic bands in fluorescence spectrum of monomeric pyrene at 383 and 372 nm, respectively, is the most sensitive of them to the polarity of local microenvironment and was used in this study to follow the complex formation of DNA and synthetic polyribonucleotides with DDA and DTAB.

The dependence of this parameter on DDA concentration both in the absence and presence of DNA is shown in Fig. 2. Practically the same course of I_3/I_1 changes is observed on DTAB concentration. For example, I_3/I_1 does not depend on the concentration of cationic amphiphile in the absence of DNA (Fig. 2A) until reaching a threshold concentration above which sharp increase in I_3/I_1 is observed passing finally to a plateau. Such behavior of I_3/I_1 on amphiphile concentration indicates to the transfer of pyrene molecules from hydrophilic aqueous surrounding into hydrophobic phase arising as the result of micelle formation by DDA and DTAB. This interpretation seems to be rather convincing because of very close coincidence of the threshold concentrations of DDA (2.5×10^{-3}M) and DTAB (1.0×10^{-2} M) obtained from the data in Fig. 2A with values of critical micelle concentration (CMC) of these amphiphiles measured by other techniques, for example, by light scattering and conductometry [60]. Taken into account the incommensurably higher solubility of pyrene in hydrophobic solvents, it can be concluded that sharp increase of I_3/I_1 with concentration of DDA and DTAB is the result of redistribution of pyrene molecules between water and hydrophobic phase of formed micelles. Reaching by I_3/I_1 of plateau values at high concentrations of DDA and DTAB (Fig. 2A) corresponds to the transition of all pyrene molecules from aqueous into hydrophobic intramicellar phase.

Much more complicated is the dependence of I_3/I_1 on DDA and DTAB concentrations when DNA is present in solution (Fig. 2B). In this case, two ranges of concentrations of cationic lipid can be marked (I and III, Fig. 2B) where sharp increase in I_3/I_1 takes place, and these are separated by an extended plateau (II), where the values I_3/I_1 remain

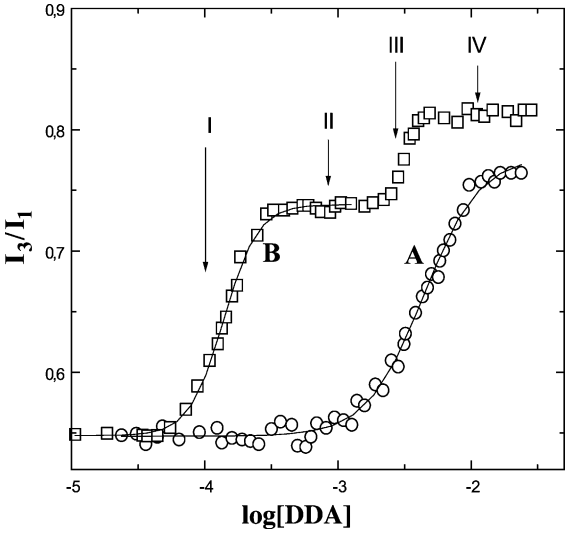

Fig. 2. Dependence of the ratio of intensities of third and first vibronic bands in fluorescence spectra of pyrene, I_3/I_1, on logarithm of DDA concentration: (A) in absence of DNA, (B) at DNA concentration equals to 4.85×10^{-5} M (per phosphate). For detailed discussion of concentrational regions I, II, III, and IV, see text.

practically unchanged. As it was pointed out above, the sharp increase of I_3/I_1 is the result of the formation in the system of micelle-like structures which solubilize pyrene molecules from aqueous surroundings. Therefore, it can be concluded that the first jump in I_3/I_1 observed, in the presence of DNA (I, Fig. 2B), at DDA and DTAB concentrations much lower of their CMC evidences the direct binding of DDA and DTAB to polynucleotide chain of DNA. This binding results in the formation of complex containing hydrophobic clusters, and the onset of I_3/I_1 increase in Fig. 2B can be considered as critical aggregation concentration (CAC). An extensive plateau (II, Fig. 2B) observed immediately after the first jump in I_3/I_1 can be interpreted as the result of the formation of stoichiometric complex of DNA with DDA and DTAB. Unfortunately, it is impossible to determine the complex stoichiometry only from pyrene fluorescence data, however, the observed in experiments deepened with time opalescence of DNA solutions at DDA and DTAB concentrations corresponding to plateau II, ending in some cases with precipitation, indicates indirectly in favour of the formation of complex with stoichiometry close to 1:1 (i.e. one molecule of cationic lipid per one negatively charged phosphate group of DNA). Exactly in this case, one can expect the lowering in solubility of the complex caused by strengthening of aggregation processes as a result of neutralization of negatively charged phosphate groups by positively charged $-NH_3^{\oplus}$ and $-N(CH_3)_3^{\oplus}$ groups upon DDA and DTAB binding to DNA. Studies of the interaction of DTAB, TTAB and CTAB with DNA using surfactant-sensitive electrode [2,16,39] as well as simple stereochemical considerations give additional arguments in favour of stoichiometry of the complex close to 1:1 at DDA and DTAB concentrations corresponding to plateau II at Fig. 2B. Strictly speaking, the stoichiometry 0.8:1 follows from direct potentiometric measurements [2,16,39] that, however, does not influence essentially on the discussions below. It is seen from Fig. 2 also that the second jump in I_3/I_1 (region III) takes place upon further increase of DDA and DTAB concentrations followed by exit into the second plateau (region IV). The range of DDA and DTAB concentrations corresponding to this transition practically coincides with that concentrational range where micelle formation of these cationic amphiphiles occurs in the absence of DNA. It would be natural to suppose that this process, i.e. independent of DNA micelle formation by DDA and DTAB, is the reason of the sharp increase in I_3/I_1 in region III. There is, however, a line of facts, including experimental ones [43], which allow us to conclude about additional binding of DDA and DTAB molecules with DNA in this region resulting in the formation of another type of DNA–cationic amphiphile complex. The structural features of complexes formed in this range of concentration have been discussed elsewhere [61], and in this paper, we limit ourselves by the physicochemical characterization of complexes with the stoichiometry close to 1:1 formed by DNA and synthetic polyribonucleotides with DDA and DTAB at concentrations of these cationic amphiphiles much lower of their CMC.

Fig. 3 demonstrates the dependence of I_3/I_1 on DDA concentration at different DNA concentrations. A consecutive increase in the absolute value of $(I_3/I_1)_{max}$ corresponding to the region of stoichiometric complex existence, i.e. plateau region, occurs with increase of DNA concentration. Seemed unclear, at first sight, the unusual fact that different values of $(I_3/I_1)_{max}$ refer to the same complex is easily explained taking into account that the measured fluorescence spectra are a superposition of signals from pyrene molecules located in different microenvironments—in aqueous phase, $(I_3/I_1)_{hydrophilic}$, and in hydrophobic clusters of formed complexes, $(I_3/I_1)_{hydrophobic}$. Therefore, the determined parameter I_3/I_1 from these spectra may be presented as a sum:

$$I_3/I_1 = \alpha(I_3/I_1)_{hydrophilic} + (1-\alpha)(I_3/I_1)_{hydrophobic} \quad (1)$$

where α and $1-\alpha$ are the molar parts of pyrene molecules located in aqueous and hydrophobic surroundings, respectively. It is quite natural that, with the increase of DNA concentration, the number of DDA molecules bound with DNA increases, which is equivalent to the extension of the volume of hydrophobic phase capable of accommodation for greater quantity of pyrene molecules. It is seen from Fig. 4 that $(I_3/I_1)_{max}$ approaches asymptotically with DNA concentration the limiting value, which can be considered as a

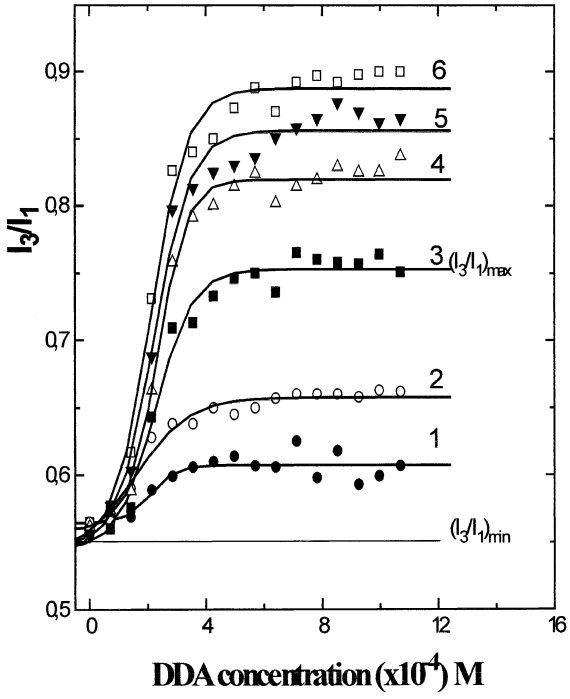

Fig. 3. The ratio of intensities of pyrene vibronic bands, I_3/I_1, versus DDA concentration at different concentrations of DNA: (1) 4.85×10^{-6} M, (2) 9.67×10^{-6} M, (3) 2.43×10^{-5} M, (4) 7.45×10^{-5} M, (5) 2.43×10^{-4} M, and (6) 4.83×10^{-4} M.

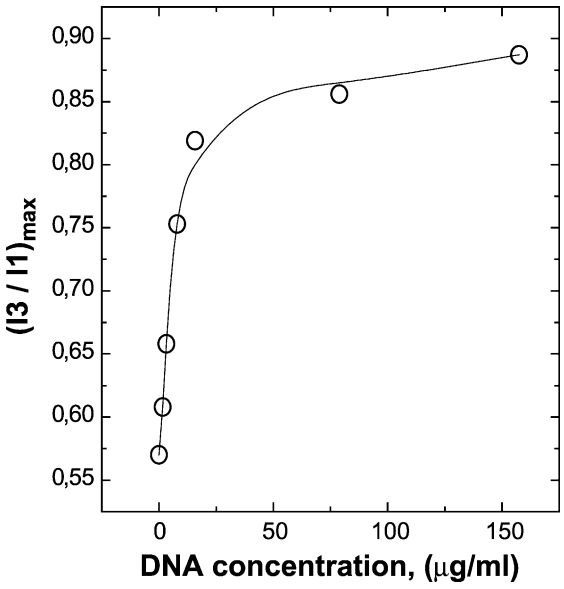

Fig. 4. I_3/I_1 versus DNA concentration (in μg/ml) at DDA concentration corresponding to the region of first plateau (region II in Fig. 2A).

measure of polarity of the medium inside hydrophobic clusters. This value equals to ~0.9, which corresponds in accordance with the known scale of hydrophobicity [51,58] to the polarity intermediate between that of ethanol and *n*-propanol. Rather high polarity of microenvironment for pyrene probe is the result either of high permeability of formed clusters for water molecules or of localization of pyrene molecules close to the surface of the clusters. It should be noted that more than two-order increase in DNA concentration (Fig. 3) practically does not effect the CAC of both DDA and DTAB, i.e. there is no shift of I_3/I_1 curves versus cationic amphiphile concentration along the *X*-axis. These data are in apparent contradiction to theoretically expected and really observed in experiments with synthetic polymers noticeable shift in CAC of cationic amphiphile to higher values with increase of polymer concentration [8,9]. Thorough analysis shows, however, that this contradiction is the exception rather than a rule, and the apparent independence of CAC on polymer concentration should always be observed when the concentration of cationic amphiphile is much higher of polymer concentration, and this is the case in our experiments (Fig. 3).

3.2. Thermodynamics of interaction of DDA and DTAB with DNA and polyribonucleotides

The model of cooperative binding of low-molecular ligands to linear polymers [62–64] was used in this study for analysis of thermodynamics of complex formation of DNA and synthetic polyribonucleotides with DDA and DTAB. This model has been fruitfully used for the analysis of various systems, such as complexes of synthetic polyelectrolytes with oppositely charged surfactants [2,16,36,37], helical structures formed by polynucleotides with complementary and non-complementary monomers [65–68] and many others. Simple conceptions lie in the foundation of this model: first—a linear row of binding sites along polymer chain, and second—two equilibrium constants for ligand binding to polymer. The first of these constants refers to binding of ligand to an isolated binding sites, and the second, to the ligand binding with the site in close neighborhood with already occupied one. As applied to our systems, the former can be treated as an equilibrium constant for electrostatic interaction of cationic amphiphile with negatively charged phosphate groups of the polynucleotide chain, K_{el}, while the latter is the product of K_{el} and the constant of hydrophobic interaction, K_h, of neighbor amphiphile molecules. Though rather simplified, this model, nevertheless, provides convenient formalism for the first approximation of the binding process. Theoretical consideration of this model gives the following analytical expression for isotherm of ligand binding with polymer:

$$\Theta = 1/2\{1 - (1 - K_{el}K_hC_f)/[(1 - K_{el}K_hC_f)^2 + 4K_{el}C_f]^{1/2}\} \quad (2)$$

where Θ is the degree of binding, and C_f is the concentration of free ligand in solution.

Two simple equations can be drawn from Eq. (2):

$$K_{el}K_h = 1/(C_f)_{\Theta=0.5} \quad \text{and} \quad (\partial\Theta/\partial C_f)_{\Theta=0.5} = \sqrt{K_h}/4 \quad (3)$$

which allow the separate determination of binding constants K_{el} and K_h from binding isotherms. The binding isotherms, which are the dependences of binding degree, Θ, on the concentration of free ligand, C_f, can easily be obtained from experimental curves like the one presented in Fig. 3 assuming the formation of complexes with stoichiometry 1:1, and determining Θ as follows:

$$\Theta = [(I_3/I_1) - (I_3/I_1)_{min}]/[(I_3/I_1)_{max} - (I_3/I_1)_{min}] \quad (4)$$

where I_3/I_1 is the measured value of parameter I_3/I_1 at different concentrations of ligand, and the meaning of $(I_3/I_1)_{min}$ and $(I_3/I_1)_{max}$ is clear from Fig. 3.

Fig. 5 shows built in this way isotherms of DDA binding with native and denatured DNA, single-stranded polyribonucleotides poly(A) and poly(U), as well as with double-helical poly(A)·poly(U). It is seen that the parameters of binding isotherms, such as the slope at the middle point ($\Theta = 0.5$), and concentration of free DDA (and DTAB) at this point are essentially dependent on the type of polynucleotide. This means that the polynucleotide chain cannot be considered as a passive template upon binding of cationic amphiphile, but on the contrary, it actively influences the process of complex formation and its thermodynamics. Equilibrium constants for binding of DDA and DTAB to different polynucleotide chains obtained from these binding isotherms are summarized in Table 1.

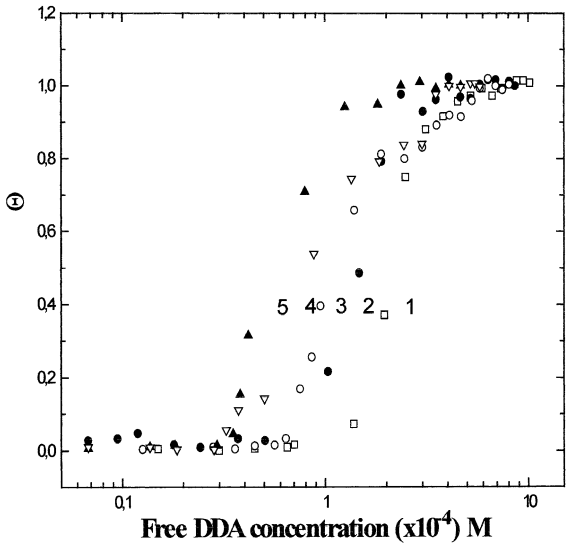

Fig. 5. Binding isotherms of DDA with native (1) and denatured (2) DNA, with single-stranded polyribonucleotides poly(U) (3), poly(A) (5), as well as with double helix poly(U)·poly(A) (4).

Several conclusions can be drawn from the analysis of the data presented in this table. Firstly, complexes of DDA with highly flexible polynucleotide chains (denatured DNA, single-stranded poly(A) and poly(U)) are characterized by rather weak hydrophobic interaction of DDA molecules ($K_h = 9.5–13$). For all complexes $K_h \gg 1$, that points to high cooperativity of interaction of DDA and DTAB with all polynucleotides ($K_h \ll 1$, $=1$, and $\gg 1$ for anti-cooperative, non-cooperative and cooperative processes, respectively [62–64]). Secondly, the hydrophobic interaction of adjacent DDA (or DTAB) molecules bound with native DNA is essentially stronger than that with single-stranded polynucleotides (K_h for native DNA is much higher than that for single-stranded poly(A) and poly(U)). It is quite possible, that an additional hydrophobic contact of aliphatic chain of cationic amphiphile with nucleic bases in the small or large groove of the double helix is responsible for this difference. It is also seen from this table that equilibrium constant for electrostatic interaction of DDA with DNA double helix and single-stranded polynucleotides, K_{el}, is much higher than the equilibrium constant for hydrophobic interaction, K_h. As it will be shown below, not only electrostatic interaction of DDA with phosphates of DNA is characteristic for unsubstituted amino groups of DDA but also their hydrogen bonding with nucleic bases, and the experimentally determined K_{el} is, in reality, an apparent constant including both of these interactions. However, hydrogen bonding seems to be much weaker than electrostatic interaction (see Table 2), and one may state that electrostatic interaction of positively charged amino groups of DDA with negatively charged phosphates of DNA makes the main contribution into the stabilization of the complex. Opposite is true for complexes of DTAB with DNA and polyribonucleotides for which noticeable prevalence of hydrophobic interaction of neighbor DTAB molecules on polynucleotide chain over electrostatic interaction of DTAB head groups with negatively charged phosphates is observed. This fact suggests that there exists close and direct contact of unsubstituted, positively charged amino groups of DDA with negatively charged phosphate groups of the ribose-phosphate backbone, possibly, strengthened by formation of hydrogen bond like $N^+—H\cdots—O—P$, whereas the contact of large methyl-substituted ammonium groups of DTAB with phosphate groups is less tighter and is, probably, realized indirectly, through molecules of bound water. Another fact which attracts attention is rather high values of K_{el} for interaction of DDA with single-stranded poly(A) and poly(U), and especially with double-helical poly(A)·poly(U). It is probable, that this effect is partly connected with high contribution to the binding process of end phosphate groups carrying the double negative charge, since relative number of the end phosphates is much higher in polyribonucleotides in comparison with DNA because of lower molecular mass of polynucleotides (mol. weight of polynucleotides is approximately 300 times lower of that for DNA).

In view of the important contribution of electrostatic interactions to the stability of the complexes, it was interesting to study the influence of monovalent cation on the thermodynamic parameters of complex formation. With this purpose, the dependencies of I_3/I_1 on DDA concentration in the presence of fixed concentration of DNA were measured at three NaCl concentrations one order differing from each other, and the binding isotherms were built in accordance with above described methodology (Fig. 6). The consec-

Table 1
Equilibrium constants of DDA and DTAB binding with native and denatured DNA, and synthetic polyribonucleotides in 10^{-2} M NaCl 10^{-3} M Tris–HCl, pH 7.2

Polynucleotide	Cationic amphiphile	K_{el}, M^{-1}	K_h
Native DNA	DDA	150	30
Denatured DNA		480	13
Poly(U)		850	9.8
Poly(A)		1210	9.5
Poly(A)·poly(U)		1708	9.6
Native DNA	DTAB	8.2	166
Denatured DNA		106	15
Poly(U)		19	62
Poly(A)		3.9	372
Poly(A)·poly(U)		7.8	205

Table 2
Thermodynamic parameters of DDA binding with native DNA in 10^{-3} M Tris–HCl, pH 7.2 at room temperature and different NaCl concentrations

NaCl concentration, M	K_{el}, M^{-1}	K_h	ΔG_{el}, kJ/mol
10^{-3}	3723	3.4	−20.6
10^{-2}	152	30	−12.5
10^{-1}	57	30	−10.1

$\Delta G_{el} = -RT\ln K_{el}$ is Gibbs' free energy for electrostatic interaction of DDA with phosphate groups of DNA.

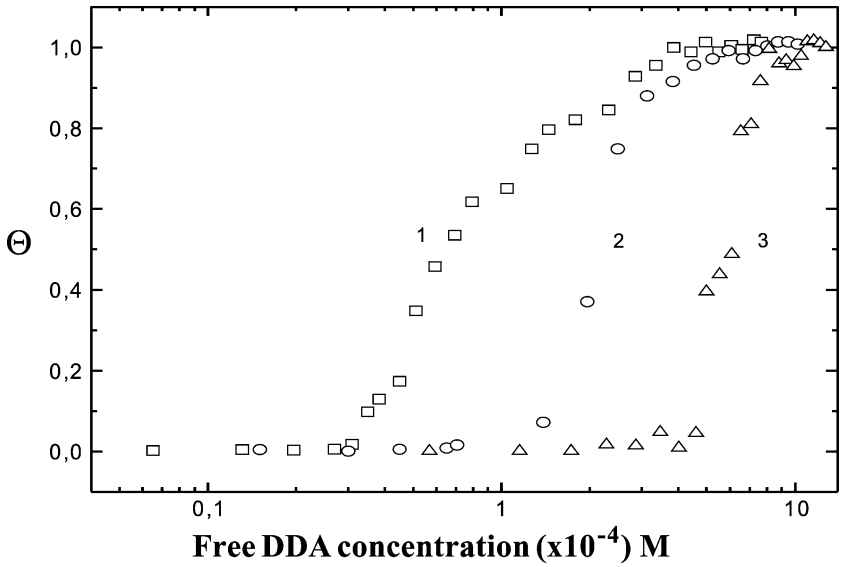

Fig. 6. Binding isotherms of DDA with native DNA at different NaCl concentrations. (1) 0.001 M, (2) 0.01 M, and (3) 0.1 M.

utive shift of isotherms of DDA binding to higher concentrations is observed with rise of $Na^{\oplus}$ concentration, which seems to be the result of a competition between $Na^{\oplus}$ and $DDA^{\oplus}$ cations for binding sites—negatively charged phosphate groups of DNA. Thermodynamic parameters of complex formation obtained from these binding isotherms are summarized in Table 2.

It is seen from this table that the increase of $Na^{\oplus}$ concentration in the medium from 10^{-3} to 10^{-1} M results in more than 50-fold lowering of the equilibrium constant for electrostatic interaction of positively charged $NH_3^{\oplus}$ groups of DDA with negatively charged phosphate groups of DNA. This is equivalent to the loss in electrostatic Gibbs' free energy of complex formation of more than in 10 kJ/mol. Very low value of K_{el} in 10^{-1} M NaCl (57 M^{-1}), which, surely, must be essentially lower in 1 M NaCl, supports the statement above about weak contribution of hydrogen bonding to the energetics of DDA interaction with nucleic acids. It is interesting that the equilibrium constant for hydrophobic interaction of DDA molecules bound at neighbor binding sites of DNA, K_h, increases nearly 10 times at transition from 10^{-3} to 10^{-1} M NaCl, and this correlates well with the known fact of strengthening of hydrophobic interactions with increasing the ionic strength of solution [69].

3.3. The influence of DDA and DTAB on UV-, CD-spectra and UV-melting curves of DNA

3.3.1. UV

We have studied in detail the effect of increasing the concentrations of DDA and DTAB on UV-spectra of DNA in the range of wavelengths 220–350 nm. All the observed in this spectral region changes may be attributed either to the change of extinction coefficient of nucleic bases as a result of structural alterations in DNA secondary structure or to the light scattering by micellar structures formed by DNA with DDA and DTAB, since neither DDA nor DTAB have any absorption bands in this region. A common feature for DDA and DTAB is a regular increase of optical density of DNA solutions with increase of concentrations of these compounds in the whole spectral range including the wave range far away from DNA absorption, i.e. at $\lambda \geq 320$ nm. The increase in optical density at $\lambda \geq 320$ nm with concentration of DDA and DTAB results from the formation of compact light scattering particles. When concentrations of

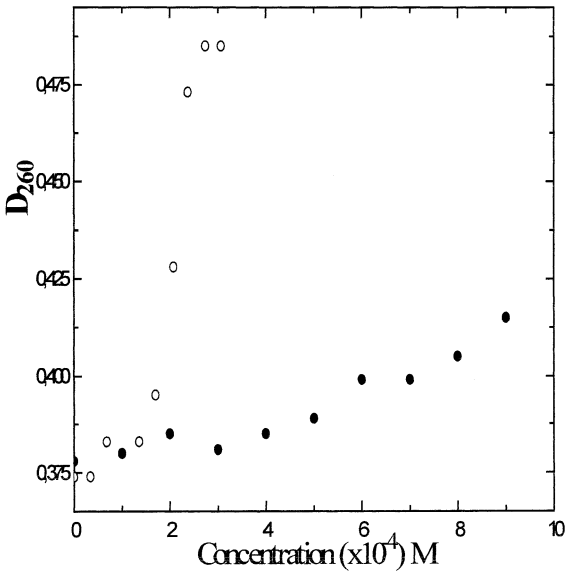

Fig. 7. The changes of optical density of DNA in maximum of absorption band (D_{260}) with concentration of DDA (○) and DTAB (●) at room temperature.

DDA and DTAB reach the values corresponding to the formation of stoichiometric complex (region II, Fig. 2), light scattering enhances as much as becomes detectable visually as opalescence of solution. The optical density at 320 nm monotonously increases with increasing the concentration of both DDA and DTAB. Quite different are the dependences of optical density on concentration of DDA and DTAB at maximum of DNA absorption ($\lambda = 260$ nm) (Fig. 7). While monotonous increase of optical absorption is retained for DTAB (Fig. 7, solid circles); such dependence for DDA is clearly sigmoidal (Fig. 7, open circles); which indicates to a specific influence of DDA on DNA secondary structure, namely, to destabilization or even partial unwinding of the double helix. To check this assumption, we have studied the influence of DDA and DTAB binding on UV-melting profile of DNA as well as on its CD- and IR-spectra.

3.3.2. UV-melting

Fig. 8 shows UV-melting curves of DNA in buffer solution and in the presence of increasing concentrations of DDA and DTAB. An increase in DTAB concentration results in consecutive shift of melting curves to higher temperatures, which indicates to the stabilizing effect of DTAB binding on DNA double helix, most likely due to the effective screening of negatively charged phosphate groups by positively charged head group of DTAB. The efficiency of this screening is high enough, it is much higher than the screening by $Na^{\oplus}$ ions, for example. It is supported by the estimations using the known formula given in Ref. [70], which show that for experimentally observed 10 °C increase in melting temperature, T_m, of DNA, it is necessary to make the concentration of $Na^{\oplus}$ in solution approximately three orders higher than the concentration of DTAB necessary for the same increase in T_m of DNA (Fig. 8A). The increase of DDA concentration, on the contrary, results to the consecutive shift of melting curves of DNA to lower temperatures (Fig. 8B), indicating to some destabilization of DNA double helix upon DDA binding.

3.3.3. CD

An additional evidence in favour of the destabilizing effect of DDA on DNA double helix comes from the analysis of the effect of DDA and DTAB on CD-spectra (not shown), which are very sensitive to any structural

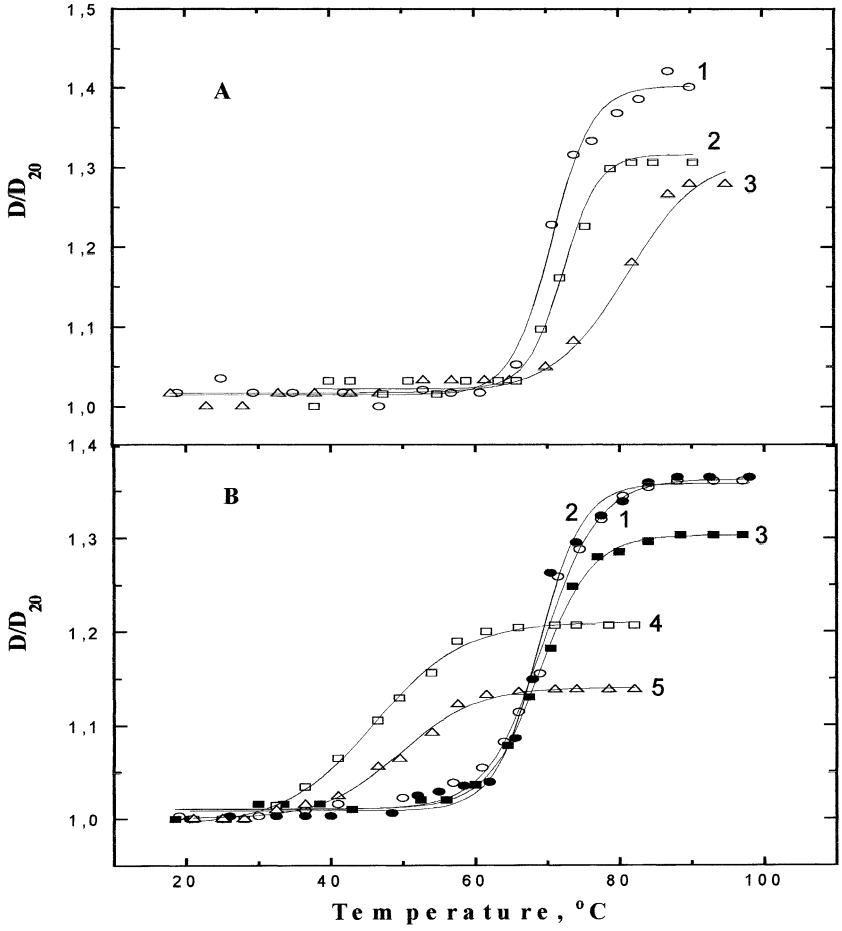

Fig. 8. UV-melting curves of DNA at different concentrations of DTAB (A) and DDA (B). DTAB concentrations: (1) 0 M, (2) 4.0×10^{-4} M, and (3) 7.0×10^{-4} M. DDA concentrations: (1) 0 M, (2) 6.3×10^{-5} M, (3) 1.0×10^{-4} M, (4) 1.7×10^{-4} M, and (5) 2.5×10^{-4} M.

changes or distortions in DNA helix. It has been demonstrated that DTAB does not practically exert any noticeable effect on the parameters of CD-spectrum while essential lowering the ellipticity both of positive and negative band is observed in the presence of DDA, which point to a partial unwinding of the double helix due to DDA binding.

3.3.4. IR

Fig. 9 demonstrates IR-spectra of DNA complexes with DDA and DTAB, as well as the spectra of native and heat denatured DNA at high relative humidity (93%). Their analysis supports the above conclusion about stabilizing effect of DTAB and destabilizing effect of DDA on DNA double helix. This follows from the observed influence of DDA and DTAB binding on selected vibrational bands of DNA at 1712, 1088, and 1053 cm^{-1}, which are known to be very sensitive to conformational state of DNA [71–73]. The band 1712 cm^{-1}, which is characteristic of native state of DNA and refers to the stretching vibration of C=O groups of guanine, cytosine and thymine in complementary base pairs in stacked state, is shifted to 1692 cm^{-1} upon helix unwinding. The narrow vibration bands at 1088 and 1053 cm^{-1}, originated from symmetric stretching vibration of phosphate groups and collective vibration of deoxyribose backbone, are widened and shifted to higher frequencies upon DNA denaturation. The comparison of IR-spectra of DNA complexes with DTAB and DDA (Fig. 9a,c) with IR-spectra of native and heat denatured DNA (Fig. 9b,d) evidences the opposite effects of DTAB and DDA on DNA—while the binding of DTAB stabilizes the double helix, the binding of DDA destabilizes it. The mechanism for such destabilization may reside in possibility for DDA carrying unsubstituted $NH_3^{\oplus}$ group to form, as opposite to DTAB, intermolecular hydrogen bonds with nucleic bases thus breaking the intramolecular H-bonding in complementary Watson–Crick A·T and G·C base pairs.

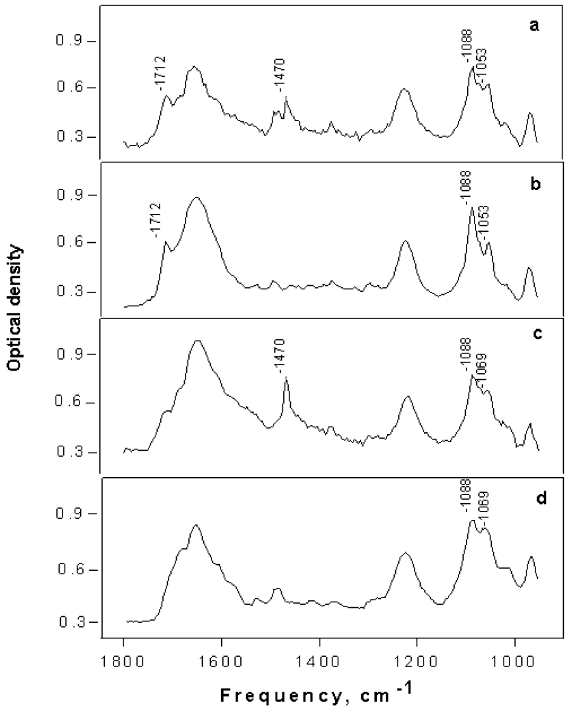

Fig. 9. IR-spectra of DNA complexes with DTAB (a), DDA (c), and native (b) and heat denatured (d) DNA at relative humidity 93%.

4. Conclusions

Thus, both common and specific features of complex formation of DDA and DTAB with nucleic acids were revealed in the present work. Among common features of these cationic amphiphiles one should mention of are the following: (i) cooperative character of binding with polynucleotide chains, (ii) the formation of two types of complexes depending on the cationic amphiphile/polynucleotide concentration ratio, (iii) a strong shift of CMC values of these compounds to lower concentrations in the presence of DNA and polynucleotides, and (iv) preferential contribution of electrostatic and hydrophobic interactions to the stability of formed complexes. The specific features of complex formation connected with different chemical structure of polar heads of DDA and DTAB one should point out are as follows: (i) two types of binding sites on polynucleotide chain for DDA, (ii) tight and direct contact of DDA amino group with negatively charged phosphate group of polynucleotide chain for DDA, and indirect, mediated by bound water molecules, contact of DTAB with phosphates, and (iii) the opposite, stabilizing (DTAB) and destabilizing (DDA) effects of these cationic amphiphiles on DNA double helix.

Several consequences follow from the results of physicochemical analysis of complex formation of DDA and DTAB with nucleic acids. First, one can state that not only an injury to functioning of biological membranes lies, as it is considered presently [13–15], in the basis of the cytotoxic effect of aliphatic amines, but their direct damaging action on genetic apparatus—DNA as well. Second, it is necessary to take into account when searching for and synthesizing new cationic lipids for high efficient DNA delivery into eukaryotic cells that the presence of unsubstituted amino groups in cationic lipid may result in destabilization, or even partial denaturation of DNA. Third, in this work, the demonstrated ability of aliphatic amines to destabilize and unwind locally the DNA double helix may play a role in complicated mechanism of initiation of template synthesis by RNA- and DNA-polymerases in the processes of DNA transcription and replication.

Acknowledgements

This work was supported by Russian Foundation for Basic Research (Grant No. 97-03-32681a) and Russian Ministry of Sciences within the frame of the program

“National priorities in medicine and biotechnology. 08. Gene therapy” (Grant No. 08.01.01.03).

References

[1] F. Evans, H. Wennerström, The Colloidal Domain: Where Physics, Chemistry, Biology and Technology Meet, VCH Publishers, New York, 1994.

[2] K. Hayakawa, J.C.T. Kwak, Interactions between polymers and cationic surfactants, in: D.N. Rubingh, P.M. Holland (Eds.), Cationic Surfactant: Physical Chemistry, Surfactant Sci. Ser., vol. 37, Marcel Dekker, New York, 1991, pp. 189–248.

[3] Y.-C. Wei, M. Hudson, The interaction between polyelectrolytes and surfactants of opposite charge, J.M.S.-Rev. Macromol. Chem. Phys. C35 (1995) 15–45.

[4] Yu.S. Tarakhovsky, G.R. Ivanitsky, Liposomes in gene therapy: structural polymorphism of lipids and efficiency of gene delivery, Biokhimiya 63 (1998) 723–736.

[5] Yu.A. Zakharova, A.D. Kolbanovsky, L.A. Krinitskaya, V.A. Kasaikin, A.M. Wasserman, Spine-probe in polymer micelles: complexes of sodium poly(acrylate) with dodecyltrimethylammonium bromide, Vysokomol. Soedin. 37 (1995) 1561–1565.

[6] J.C. Brackman, J.B.F.N. Engberts, Polymer–micelle interactions: physical organic aspects, Chem. Soc. Rev. 22 (1993) 85–92.

[7] M.J. Lowrence, Surfactant systems: their use in drug delivery, Chem. Soc. Rev. 23 (1994) 417–424.

[8] P. Hansson, M. Almgren, Large C_{12}TAB micelles formed in complexes with polyvinylsulfate and dextran sulfate, J. Phys. Chem. 99 (1995) 16694–16703.

[9] P. Hansson, M. Almgren, Interaction of C_nTAB with sodium (carboxymethyl)cellulose: effect of polymer linear charge density on binding isotherms and surfactant aggregation number, J. Phys. Chem. 100 (1996) 9038–9046.

[10] S. Bhattacharya, S.S. Mandal, Evidence of interlipidic ion-pairing in anion induced DNA release from cationic amphiphile–DNA complexes. Mechanistic implications in transfection, Biochemistry 37 (1998) 7764–7777.

[11] S.Z. Bathaie, A.A. Moosavi-Movahedi, A.A. Saboury, Energetic and binding properties of DNA upon interaction with dodecyltrimethylammonium bromide, Nucleic Acids Res. 27 (1999) 1001–1005.

[12] B. Bhattacharya, S.S. Mandal, Interaction of surfactants with DNA. Role of hydrophobic and surface charge in intercalation and DNA melting, Biochim. Biophys. Acta 1323 (1997) 29–44.

[13] A. Albert, Selective toxicity, The Physico-Chemical Basis of Therapy, Chapman and Hall, London, 1985.

[14] A.N. Wievsky, Mechanisms of Biological Effect of Surface-Active Substances, Nauka, Moscow, 1991.

[15] D.L. Fredel, Biological applications of cationic surfactants, in: J. Cross, E.J. Singer (Eds.), Cationic Surfactants. Analytical and Biological Evaluation, Marcel Dekker, New York, 1994, pp. 31–60.

[16] S.V. Mel’nikov, V.G. Sergeev, K. Yoshikawa, Transition of double-stranded DNA chains between random coil and compact globule states induced by cooperative binding of cationic surfactant, J. Am. Chem. Soc. 117 (1995) 9951–9956.

[17] O.A. Pyshkina, V.G. Sergeev, A.V. Lezov, S.V. Mel’nikov, E.I. Rumtsev, A.V. Zezin, V.A. Kabanov, Compact form of the complex DNA–cationic surfactant in chloroform, Doklady RAN 349 (1996) 772–775.

[18] D.G. Knorre, V.V. Vlassov, Cell membranes as a barrier in the biological applications of antisense oligonucleotides, their derivatives and analogs, Bioorg. Khim. 18 (1992) 1330–1340.

[19] B.I. Sukhorukov, V.V. Kuvichkin, L.I. Shabarchina, On the structure and function of DNA–membrane contact in a cell, Biofizika 25 (1980) 270–275.

[20] P. Mitrakos, P.M. McDonald, Cationic amphiphile interactions with polyadenylic acid as probed via ^{2}H-NMR, Biochim. Biophys. Acta 1374 (1998) 21–33.

[21] M.P. Moyer, The association of DNA and RNA with membranes, Int. Rev. Cyt. 61 (1980) 1–61.

[22] V.A. Struchkov, N.B. Strazhevskaya, DNA-bound lipids: composition and possible functions, Biokhimiya 58 (1993) 1154–1175.

[23] R.I. Zhdanov, V.V. Kuvichkin, Membrane phospholipids act as DNA/RNA receptors during formation of specific DNA nuclear membrane contacts and gene expression. A hypothesis based on the study of interaction between phospholipid vesicles and DNA or polynucleotides, in: J.A. Gustafson, K.W.A. Wirtz (Eds.), New Developments in Lipid–Protein Interactions and Receptor Function, Plenum, New York, 1993, pp. 249–261.

[24] V.V. Kuvichkin, Lipid–nucleic acid interactions in vitro and in vivo, Usp. Sovrem. Biol. 120 (2000) 466–476.

[25] G.B. Sukhorukov, M.M. Montrel, A.I. Petrov, L.I. Shabarchina, B.I. Sukhorukov, Multilayer films containing immobilized nucleic acids. Their structure and possibilities in biosensor applications, Biosens. Bioelectron. 11 (1996) 913–922.

[26] M.M. Montrel, G.B. Sukhorukov, A.I. Petrov, L.I. Shabarchina, B.I. Sukhorukov, Spectroscopic study of thin multilayer films of the complexes of nucleic acids with cationic amphiphiles and polycations: their possible use as sensor elements, Sens. Actuators 42 (1997) 225–231.

[27] D.D. Lasic, Liposomes in Gene Delivery, CRC Press, New York, 1997.

[28] J.H. Felgner, R. Kumar, C.N. Sridhar, C.J. Wheeler, Y.J. Tsai, R. Border, P. Ramsey, M. Martin, P.L. Felgner, Enhanced gene delivery and mechanisms studies with a novel series of cationic lipid formulations, J. Biol. Chem. 269 (1994) 2550–2561.

[29] H.E.J. Hofland, L. Shephard, S.M. Sullivan, Formation of stable cationic lipid/DNA complexes for gene transfer, Proc. Natl. Acad. Sci. U. S. A. 93 (1996) 7305–7309.

[30] W.R. Jarnagin, R.J. Debs, S.-S. Wang, D.M. Bissell, Cationic lipid mediated transfection of liver cells in primary culture, Nucleic Acids Res. 20 (1992) 4205–4211.

[31] W.F. Anderson, Human gene therapy, Nature 392 (1998) 25–30 (Suppl.).

[32] H. Gershon, R. Ghirlando, S.B. Guttman, A. Minsky, Mode of formation and structural features of DNA–cationic liposome complexes used for transfection, Biochemistry 32 (1993) 7143–7151.

[33] F.M.P. Wong, D.L. Reimer, M.B. Bally, Cationic lipid binding to DNA: characterization of complex formation, Biochemistry 35 (1996) 5756–5763.

[34] S.J. Eastmen, C. Siegel, J. Tousignant, A.E. Smith, S.H. Cheng, D.K. Scheule, Biophysical characterization of cationic lipid–DNA complexes, Biochim. Biophys. Acta 1325 (1997) 41–62.

[35] R.I. Zhdanov, N.V. Semenova, A.I. Archakov, Realities and hopes of gene therapy, Vopr. Med. Khim. 46 (2000) 197–201.

[36] K. Shirahama, K. Takashima, N. Takisawa, Interaction between dodecyltrimethylammonium chloride and DNA, Bull. Chem. Soc. Jpn. 16 (1987) 43–47.

[37] K. Hayakawa, J.P. Santerre, J.C.T. Kwak, The binding of cationic surfactants by DNA, Biophys. Chem. 17 (1983) 175–181.

[38] R. Chatterjee, D.K. Chattoraj, Hydrophobic interactions of DNA with long-chain amines, Biopolymers 18 (1979) 147–166.

[39] S.V. Mel’nikov, V.G. Sergeev, K. Yoshikawa, Discrete coil-globule transition of large DNA induced by cationic surfactant, J. Am. Chem. Soc. 117 (1995) 2401–2408.

[40] C.H. Spink, J.B. Chaires, Thermodynamics of binding of a cationic lipid to DNA, J. Am. Chem. Soc. 119 (1997) 10920–10928.

[41] A.V. Gorelov, E.V. Kudryashov, J.-C. Jacquier, D.M. McLoughlin, K.A. Dawson, Complex formation between DNA and cationic surfactant, Physica, A 249 (1998) 216–225.

[42] B.I. Sukhorukov, R.L. Kazaryan, A.I. Petrov, The influence of conformational state of DNA on its complex formation with cetyltrimethylammonium bromide, Russ. J. Phys. Chem. 72 (1998) 1528–1530.

[43] B.I. Sukhorukov, R.L. Kazaryan, A.I. Petrov, G.B. Sukhorukov, Dual, stabilizing and destabilizing, effect of decylamine on DNA structure and stability, Biofizika 43 (1998) 427–432.

[44] R. Chatterjee, D.K. Chattoraj, Thermal transition of DNA in presence of long-chain amines, Indian J. Biochem. Biophys. 16 (1979) 236–239.
[45] J.-C. Jacquier, A.V. Gorelov, D.M. McLoughlin, K.A. Dawson, Capillary electrophoretic study of the complex formation between DNA and cationic surfactants, J. Chromatogr., A 817 (1998) 263–271.
[46] S. Morrissey, E.D. Kudryashov, K.A. Dawson, V.A. Buckin, Surfactant–DNA complexes in low ionic strength dilute solutions, Prog. Colloid & Polym. Sci. 112 (1999) 71–75.
[47] V. Buckin, E. Kudryashov, S. Morrissey, T. Kapustina, K. Dawson, Do surfactants form micelles on the surface of DNA? Prog. Colloid & Polym. Sci. 110 (1998) 214–219.
[48] M.V. Pattarkine, K.N. Ganesh, DNA–surfactant interactions: coupled cooperativity in ligand binding leads to duplex stabilization, Biochem. Biophys. Res. Commun. 263 (1999) 41–46.
[49] V.G. Sergeev, S.V. Michailenko, O.A. Pushkina, I.V. Yaminsky, K. Yoshikava, How does alcohol dissolve the complex of DNA with a cationic surfactant, J. Am. Chem. Soc. 121 (1999) 1780–1785.
[50] S. Mel'nikov, M.O. Khan, B. Lindman, B. Jönsson, Phase behavior of single DNA in mixed solvents, J. Am. Chem. Soc. 121 (1999) 1130–1136.
[51] K. Kalyanasundaram, J.K. Thomas, Environmental effects on vibronic band intensities in pyrene monomer fluorescence and their application in studies of micellar systems, J. Am. Chem. Soc. 99 (1977) 2039–2044.
[52] G.E. Dobretsov, Fluorescent Probes in Studies of Cells, Membranes and Lipoproteins, Nauka, Moscow, 1989.
[53] H. Itoh, S. Ishido, M. Nomura, T. Hayakawa, S. Mitaku, Estimation of the hydrophobicity in microenvironment by pyrene fluorescence measurements: *n*-octylglucoside micelles, J. Phys. Chem. 100 (1996) 9047–9053.
[54] P.O.P. Ts'o, P. Lu, Interactions of nucleic acids: I. Physical binding of thymine, adenine, steroids, and aromatic hydrocarbons to nucleic acids, Proc. Natl. Acad. Sci. U. S. A. 51 (1964) 17–24.
[55] B. Janic, Physico-Chemical Characteristics of Oligonucleotides and Polynucleotides, IFI/Plenum, New York, 1971.
[56] L.I. Shabarchina, M.M. Montrel, G.B. Sukhorukov, I.V. Savintsev, B.I. Sukhorukov, Manufacturing the multilayer DNA–cationic amphiphile films by sequential adsorbtion method and the study of their structure, Russ. J. Phys. Chem. 74 (2000) 2093–2100.
[57] G. Decher, Fuzzy nanoassemblies: toward layered polymeric multicomposites, Science 277 (1997) 1232–1237.
[58] D.C. Dong, M.A. Winnik, The Py scale of solvent polarities. Solvent effects on the vibronic fine structure of pyrene fluorescence and empirical correlation with E_T and Y values, Photochem. Photobiol. 35 (1982) 17–21.
[59] J.R. Lakowicz, Principles of Fluorescent Spectroscopy, Plenum, New York, 1983.
[60] A.A. Abramson, Surface-Active Substances, Khimiya, Leningrad, 1981.
[61] B.I. Sukhorukov, A.I. Petrov, R.L. Kazaryan, V.V. Kuvichkin, Fluorescent study of complex formation between DNA and cationic amphiphilic molecules, Biofizika 45 (1999) 239–247.
[62] G. Schwarz, Cooperative binding to linear biopolymers: 1. Fundamental static and dynamic properties, Eur. J. Biochem. 12 (1970) 442–453.
[63] K.S. Schmitz, J.M. Schurr, Cooperative binding of adenosine by polyuridylic acid: a further analysis, Biopolymers 9 (1970) 697–715.
[64] I. Satake, J.T. Yang, Interaction of sodium decylsulfate with poly (L-ornithine) and poly(L-lysine), Biopolymers 15 (1976) 2263–2275.
[65] A.I. Petrov, Complex formation between spin-labeled polyuridylic acid and pyrimidine nucleosides, Nucleic Acids Res. 8 (1980) 5913–5929.
[66] M.T. Sarocchi, Y. Courtois, W. Guschlbauer, Protonated polynucleotide structures. Specific complex formation between polycytidylic acid and guanosine or guanylic acids, Eur. J. Biochem. 14 (1970) 411–421.
[67] R.J.H. Davies, N. Davidson, Base pairing equilibria between polynucleotide and complementary monomers, Biopolymers 10 (1971) 1455–1479.
[68] R.J.H. Davies, Complexes of poly(adenylic acid) with complementary monomers, Eur. J. Biochem. 61 (1976) 225–236.
[69] C. Tanford, The Hydrophobic Effect: Formation of Micelles and Biological Membranes, Wiley, New York, 1980.
[70] J. Marmur, P. Doty, Determination of the base composition of deoxyribonucleic acid from its thermal denaturation temperature, J. Mol. Biol. 5 (1962) 109–118.
[71] M. Tsuboi, Application of infrared spectroscopy to structure studies of nucleic acids, Appl. Spectrosc. Rev. 3 (1969) 45–90.
[72] K.C. Lu, E.W. Prohovsky, A. van Zandt, Vibrational modes of A-DNA, B-DNA, and A-RNA backbones: an application of a Green-function refinement procedure, Biopolymers 16 (1977) 2491–2506.
[73] M.A. Semenov, B.I. Sukhorukov, V.Ya. Maleev, Are nucleic bases hydrated in DNA at low relative humidities? Biofizika 26 (1981) 979–984.